A&A 453, 895–902 (2006)
DOI: 10.1051/0004-6361:20054343

Astronomy & Astrophysics

[Fe/H] derived from the light curves of RR Lyrae stars in the Galactic halo⋆

C. Wu, Y. L. Qiu, J. S. Deng, J. Y. Hu, and Y. H. Zhao

National Astronomical Observatories, Chinese Academy of Sciences, Beijing 100012, PR China
e-mail: [wuchao;yzhao]@lamost.org;[qiuyl;jsdeng;hjy]@bao.ac.cn

Received 12 October 2005 / Accepted 3 March 2006

ABSTRACT

Context. The iron abundance of halo RR Lyrae stars can provide important information about the formation history of the Galactic halo.
Aims. We determine the [Fe/H] of the sample of halo RRab stars by using the P-φ_{31}-[Fe/H] relation developed by Jurcsik & Kovács based on their light curves. We need to extend the relation from the V band to our unfiltered CCD band.
Methods. To do this, we use the low-dispersion spectroscopic [Fe/H] of literatures and the photometric data released by the first-generation Robotic Optical Transient Search Experiment (ROTSE-I) project. We do regression analyses for the *calibrating sample* using a linear function and test its validity by comparing of the predicted [Fe/H] with the spectroscopic [Fe/H]. In general, the fit accuracy for the two different [Fe/H] is better than 0.19 dex.
Results. We derive an empirical P-φ_{31}-[Fe/H] linear relation for the unfiltered CCD band (ROTSE-I), i.e. [Fe/H] = $-3.766 - 5.350$P$+1.044\varphi_{31}$. In our test, the P-φ_{31}-[Fe/H] relation is also fit for our unfiltered CCD band. In addition, another linear relation, $\varphi_{31\_V} = 0.882 + 0.792\varphi_{31\_W}$, is also derived for the transformation between the V and W bands. We present the predicted [Fe/H] of the sample (the 31 halo RRab stars) in a catalog.
Conclusions. The mean [Fe/H] of the sample is −1.63 with dispersion of 0.45 dex in distribution, which is consistent with the results derived from the blue horizontal branch star candidates by Kinnman et al. (2000, A&A, 364, 102). The mean [Fe/H] values of the RRab stars in the range of 1 kpc, 2 kpc, and 3 kpc from the star 91 (a double-mode RR Lyrae star), are all lower than that of the background halo stars. These values are consistent with that of star 91 suggested by Wu et al. (2005, AJ, 130, 1640), which indicates they might have a common origin.

Key words. Galaxy: halo – stars: variables: RR Lyr – Galaxy: abundances

1. Introduction

The Solan Digital Sky Survey (SDSS) and the Quasar Equatorial Survey Team(QUEST) are broadening our understanding of the formation and evolution of the Galaxy (Newberg et al. 2002; Zinn et al. 2004). There is a lot of evidence now that the accretion of satellite galaxies has played a major role in the formation of the halo, and possibly also that of the whole Milky Way (Odenkirchen et al. 2001; Vivas et al. 2001, 2005; Yanny et al. 2000, 2003).

Ivezić et al. (2000) selected 148 candidate RR Lyrae stars (RRLSs) from ∼930 000 SDSS stars in ∼100 deg^2 of sky. Their sample shows a "45 kpc clump" in the spatial distribution, which was suspected to be a Sagittarius (Sgr) tidal stream. Constraining the sample to radii less than 35 kpc, to exclude the clump, the volume was found to follow a power law dependence on the Galactocentric radius, $R^{-3.1\pm0.2}$, in agreement with the result from the larger halo RRLSs compiled by Wetterer & McGraw (1996). The sample was enlarged by the QUEST survey (Vivas et al. 2001, 2004) and some small clumps have been detected (Vivas & Zinn 2003). Vivas et al. (2005) measured iron abundance and radial velocity for 16 stars of the "45 kpc clump" and confirmed that they are debris from the Sgr dwarf spheroidal (dSph) galaxy, using the mean [Fe/H] value of field the blue horizontal branch (BHB) star candidates to represent that of background halo stars.

Wu et al. (2005, hereafter W05) measured 71 candidates of the Ivezić et al. (2000) sample, confirmed that 69 are true RRLSs, and measured their light curves, periods, and amplitudes. We propose to measure the iron abundances of the W05 sample, which is near the Sgr tidal stream, to provide a reliable reference to the "45 kpc clump". In addition, the metallicity of these halo stars contains useful physical information about the Galactic halo.

The metallicity of RRLSs can be determined by applying the method of Fourier parameters on their light curves and periods. This method was developed by Simon (1988) and updated by Kovács & Zsoldos (1995), Jurcsik & Kovács (1996), Sandage (2004), and Kovács (2005). These authors demonstrated that certain combinations of the first few terms of a Fourier series representation of RR Lyrae light curves correlate with metallicity and period. The linear formula proposed by Jurcsik & Kovács (1996, hereafter JK96), employing the period P and the Fourier phase φ_{31} measured in the V band, is able to predict the spectroscopically observed [Fe/H] values within a standard deviation of 0.13 dex. It has been tested by Kovács (2005, hereafter K05) for a larger sample. Furthermore, Sandage (2004) can derive the P-φ_{31}-[Fe/H] relation on the basis of other empirical relations.

⋆ Figures 1 to 4 are only available in electronic form at http://www.edpsciences.org

The P-φ_{31}-[Fe/H] relation of JK96 must be extended to the unfiltered CCD band used by W05, which is similar to the R band. To do this, we use the data released by the first-generation Robotic Optical Transient Search Experiment (ROTSE-I) project, which was operated without any filter and has an effective band similar to that of W05 (Pojmanski 2002, 2003; Pojmanski & Maciejewski 2004; Woźniak et al. 2004). We can find an empirical P-φ_{31}-[Fe/H] linear relation for the unfiltered CCD band, similar to that of JK96 for the V band. This is not unexpected since φ_{31} in different optical bands has possible linear relations (Dorfi & Feuchtinger 1999; Feuchtinger 1999; Kovács & Kanbur 1998).

In Sect. 2, we describe the database groups and data reduction. In Sect. 3, we derive the P-φ_{31}-[Fe/H] relation calibrated for the unfiltered CCD band and compare it with that of JK96. In Sect. 4, we calculate the iron abundances of 31 RRLSs of the W05 sample using the calibrated relation and analyze the characteristics of these halo stars. Our results are summarized in Sect. 5.

2. Data description

Our database consists of three data sets. Data set #1 is used to search and calibrate the P-φ_{31}-[Fe/H] relation, which is tested by data set #2. Data set #3 contains 31 Galactic halo RRLSs from the W05 sample. The calibrated P-φ_{31}-[Fe/H] relation is used to predict the [Fe/H] of data set #3.

2.1. Data sets #1 and #2

We chose the data in sets #1 and #2 from the data of the Northern Sky Variability Survey (NSVS)[1] when it was first released. The NSVS online database contains four columns, i.e. MJD (epoch), magnitude, photometric error, and flag, for each variable. The NSVS was conducted in the course of ROTSE-I, primarily covering the entire northern sky to a unfiltered magnitude of 15.5 and providing between 100 and 400 good measurements per object (Woźniak et al. 2004). Its effective unfiltered CCD band is similar to the Johnson R band.

We found 46 RRLSs that are also in the sample of JK96 and marked them as set #1. Our set #2 includes 72 RRLSs that have spectroscopic [Fe/H] (Layden 1994, hereafter L94), except those already included in set #1. To ensure the photometric accuracy of the light curves, RRLSs fainter than 13 mag in the V band and those south to *declination* $= -10^\circ$ were not selected. As a result, the data that we selected have a mean accuracy better than 0.05 mag, according to Woźniak et al. (2004). On average, the observations spanned a period of about one year.

2.2. Data reduction

Periods were found for the time series M(t) using the Phase Dispersion Minimization (PDM) technique as implemented in IRAF[2] (Stellingwerf 1978). We searched for periods on the interval 0.1 day $< P <$ 1 day and investigated in detail any minima in the θ statistic that appeared significant. We gave special scrutiny to the region within ±10% of the period listed in the Combined General Catalogue of Variable Stars (GCVS4; Kholopov 1988; Durlevich 1994). The value of $P_{\rm GCVS4}$ is helpful in locating a period when the time coverage of these data did not strongly constrain the period. The subharmonics were distinguishable using the method mentioned in W05. Generally, we chose the period that produced the light curve with the least scatter.

Fourier decompositions were performed for the light curves folded by PDM, following K05 and using the definition in Kovács & Zsoldos (1995), i.e.

$$M = A_0 + \sum_{i=1}^{N} A_i \sin(\mathrm{i}\omega(t - t_0) + \varphi_i). \quad (1)$$

We discarded the outliers at the 3σ level and repeated the Fourier fit until no outliers were found.

Because the data are not uniformly distributed in phase, to avoid overfitting noisy light curves and underfitting those with low noise, we had to determine the Fourier order N that would yield the best result. After manual experiments, we constrained N to the range of $m - 2 \leqq N \leqq m + 2$, where m is computed by the experiential equation of K05, i.e.

$$m = \begin{cases} 4 & \text{if } m^\star < 4 \\ m^\star & \text{if } 4 \le m^\star \le 10 \\ 10 & \text{if } m^\star > 10. \end{cases}$$

The meaning of $m^\star$ is the same as that given in K05, i.e. $m^\star = INT(SNR/10)$ (see K05 for details). We searched this region for the best N using the R-Square and the root mean square error (RMSE) statistics[3]. We also visually checked whether the shape of the fitted light curve was reasonable.

The φ_{31} was calculated based on the definition of Simon & Lee (1981), i.e. $\varphi_{31} = \varphi_3 - 3\varphi_1$. The result was normalized to the range of 0 to 2π to remove the 2π ambiguity.

2.3. Data set #3

Data set #3 contains 31 RRab variables that we selected from the sample of 57 RRab stars in W05. We applied the Fourier fitting method described above to the 57 stars and discarded those with maximum R-Square value less than 0.9 and those with minimum RMSE more than 0.06. The remaining 31 halo stars have distances between 5.7 kpc and 28 kpc from the Galactic plane.

2.4. Data table

We list the variable names/IDs, periods, φ_{31}, and iron abundance of the sets #1, #2, and #3 in Tables 1–3, respectively. The folded light curves with the corresponding Fourier fits are displayed in Figs. 1–4.

The derived periods listed in Tables 1 and 2 are in good agreement with those of GCVS4 in $\sigma \sim 10^{-4}$ days, except for DG Hya. Its period in GCVS4 and ours differ by ~0.32 days. Although we also detected the period in GCVS4 (0.429973 days), the light curve is noisier than that of the period adopted here (0.753970 days). We suggest the GCVS4 period is a spurious period. This is also supported by the computation for the two various periods using Eq. (4) in Vivas et al. (2004). The periods listed in Table 3 are adopted from W05.

[1] http://skydot.lanl.gov/nsvs/nsvs.php

[2] IRAF is distributed by the National Optical Astronomy Observatory.

[3] R-Square is the square of the multiple correlation coefficient. It takes on any value between 0 and 1, with a value closer to 1 indicating a better fit. RMSE is the fit standard error. A RMSE value closer to 0 indicates a better fit.

Table 1. Set #1: ROTSE-I variables common with those in compilation of JK96.

Star	Period (d)	φ_{31}	[Fe/H]	Star	Period (d)	φ_{31}	[Fe/H]	Star	Period (d)	φ_{31}	[Fe/H]
XX And	0.722892	5.64487	–1.69	BB Eri	0.569875	5.28691	–1.32	♯RX Cet	0.573449	5.82426	–1.2
SW Aqr	0.459272	4.96191	–1.14	RR Gem	0.397269	5.26756	–0.14	♯AA Leo	0.598563	4.99218	–1.21
SX Aqr	0.535748	4.91896	–1.55	VX Her	0.455332	4.92637	–1.21	♯VY Lib	0.533404	5.61394	–1.06
BO Aqr	0.693934	5.66499	–1.52	VZ Her	0.440325	4.86611	–0.8	♯V445 Oph	0.397044	5.73612	0.01
BR Aqr	0.481782	5.44115	–0.6	SV Hya	0.478595	4.90845	–1.43	♯AR Per	0.425531	5.69689	–0.14
CP Aqr	0.463398	5.40211	–0.5	ST Leo	0.477959	5.09023	–0.98	♯RY Psc	0.529497	5.53738	–1.18
DN Aqr	0.633917	5.63168	–1.36	TV Leo	0.672885	5.26225	–1.86	♯V440 Sgr	0.477566	5.19756	–1.21
AA Aql	0.361821	5.08321	–0.27	V LMi	0.543888	5.35767	–0.93	♯UU Vir	0.475606	5.34802	–0.6
TZ Aur	0.391639	5.15205	–0.62	U Lep	0.581236	4.86869	–1.67	♯AV Vir	0.656954	5.77266	–1.02
TW Boo	0.532293	5.18551	–1.15	TT Lyn	0.597413	5.43315	–1.5	♯FH Vul	0.405541	4.41535	–0.61
W CVn	0.551739	5.32863	–0.91	IO Lyr	0.577164	5.33299	–1.1	* V341 Aql	0.578302	5.08152	–0.92
RR Cet	0.552996	5.33238	–1.29	ST Oph	0.450383	5.14435	–1.02	* RZ Cet	0.510606	5.25459	–1.24
S Com	0.586574	5.30487	–1.64	V452 Oph	0.557153	5.02819	–1.45	* BK Dra	0.592080	5.07697	–1.83
DX Del	0.472685	5.77432	–0.32	AV Peg	0.390106	5.72178	0.08	* AN Ser	0.522001	6.06785	0.09
SU Dra	0.660300	5.44729	–1.56	AT Ser	0.746538	5.65698	–1.8	···	···	···	···
RX Eri	0.587272	5.67619	–1.07	♯X Ari	0.650811	4.86683	–2.1	···	···	···	···

Notes: A pound sign in the "Star" column indicates a star with a bad quality light curve, i.e. insufficient-phase-coverage or noisy light curves. Asterisks in the "Star" columns indicate the the peculiar variables of JK96; the column "[Fe/H]" shows spectroscopic iron abundance as it was given in JK96.

Table 2. Set #2: ROTSE-I variables separate from those in the compilation of JK96.

Star	Period (d)	φ_{31}	[Fe/H]	Star	Period (d)	φ_{31}	[Fe/H]	Star	Period (d)	φ_{31}	[Fe/H]
CI And	0.484606	5.66719	–0.59	⋆DG Hya	0.753970	5.77162	–1.16	RX CVn	0.540079	5.18399	–1.05
DR And	0.563188	5.35783	–1.22	⋆ET Hya	0.685569	5.60043	–1.42	SV CVn	0.668644	4.85594	–1.91
BT Aqr	0.406340	5.63346	–0.08	GO Hya	0.636418	6.00096	–0.59	SW CVn	0.441704	4.86233	–1.26
ST Boo	0.622369	5.59893	–1.58	CQ Lac	0.620043	5.35337	–1.75	WY Dra	0.588934	5.32478	–1.39
SW Boo	0.513502	4.96241	–0.87	TW Lyn	0.481823	5.03874	–0.98	AE Dra	0.602681	5.20047	–1.27
UU Boo	0.456958	4.86037	–1.64	RR Lyr	0.566687	5.38834	–1.11	BK Eri	0.548073	4.62920	–1.37
UY Boo	0.650816	5.47849	–2.18	RZ Lyr	0.511343	4.50126	–1.84	AF Her	0.630370	5.29680	–1.66
RW Cnc	0.547221	4.84977	–1.25	CN Lyr	0.411376	5.75957	–0.05	AG Her	0.649425	5.27006	–1.72
AQ Cnc	0.548550	5.29419	–1.26	VV Peg	0.488410	4.80447	–1.60	CW Her	0.623887	5.41295	–1.80
Z CVn	0.653850	5.30675	–1.69	BH Peg	0.640348	5.49400	–1.12	GY Her	0.524397	5.23737	–1.64
RZ CVn	0.567387	5.12580	–1.64	CG Peg	0.467071	5.56699	–0.26	V394 Her	0.436072	4.93431	–1.22
SS CVn	0.478543	5.02100	–1.25	DZ Peg	0.607346	5.40118	–1.25	GL Hya	0.506045	5.39414	–1.19
UZ CVn	0.697831	5.52769	–2.04	AR Ser	0.575422	5.52688	–1.50	WW Leo	0.602278	5.73415	–1.22
AL CMi	0.550431	6.14393	–0.61	CS Ser	0.526805	4.73872	–1.30	CX Lyr	0.616751	5.29741	–1.51
TV CrB	0.584612	4.94879	–2.03	RV UMa	0.468027	5.11700	–0.94	FN Lyr	0.527380	4.84703	–1.72
XZ Cyg	0.466643	5.03771	–1.25	AB UMa	0.599607	6.01653	–0.49	V964 Ori	0.504647	5.19814	–1.61
DM Cyg	0.419969	5.56945	0.07	⋆UV Vir	0.586579	5.63595	–0.94	AE Peg	0.496717	4.53624	–1.56
CK Del	0.442746	4.83400	–1.01	⋆BQ Vir	0.637019	6.04931	–1.06	AW Ser	0.597235	5.00084	–1.40
XZ Dra	0.476426	5.30817	–0.63	BK And	0.421646	5.64058	0.28	BH Ser	0.434566	4.96517	–1.32
SZ Gem	0.501293	4.80544	–1.53	SZ Boo	0.522831	5.16030	–1.41	DF Ser	0.437775	5.17141	–0.51
DL Her	0.591588	5.35728	–1.06	RZ Cam	0.480467	4.94726	–0.77	SS Tau	0.369973	5.45369	–0.07
⋆SZ Hya	0.537317	5.15871	–1.47	AN Cnc	0.542858	5.06864	–1.19	U Tri	0.447264	5.08390	–0.56
UU Hya	0.523820	4.95565	–1.38	AS Cnc	0.617470	5.32264	–1.61	AE Vir	0.633979	5.67195	–0.91
DD Hya	0.501612	5.38029	–0.76	RR CVn	0.558575	5.13411	–0.83	FK Vul	0.434078	5.44290	–0.71

Notes: Asterisks in the "star" column indicate stars also in set #2 of K05; the column "[Fe/H]" shows the spectroscopic iron abundance in the scale of JK96, transformed from L94.

For data set #1, we selected bad quality light curves, as those with $RMSE > 0.06$, or seriously insufficient phase coverage and marked them with the symbol pound in Table 1. We also marked the peculiar stars in JK96 with asterisks. Only the remaining 31 stars are used below to determine the P-φ_{31}-[Fe/H] relation and hence are named the *calibrating sample*.

The [Fe/H] values in Table 1 are the same as those given in JK96, whose the results of several abundance measurements were combined. The abundances in Table 2 are transformed from L94 using Eq. (2) from JK96. The symbol star in this table represents the variables that also exist in K05. Table 3 lists the [Fe/H] predicted in this work, transformed to the scale of L94, and the error (see Sect. 4).

3. The P-φ_{31}-[Fe/H] relation

3.1. Calibration in the W band

JK96 have found a linear relation among the [Fe/H], period, and φ_{31} for V-band observations, which was confirmed by K05 using the extended sample of All Sky Automated Survey (ASAS). However, it has not been determined if a similar

Table 3. Set #3: SDSS RR Lyrae stars in the Galactic halo.

ID	Period (d)	φ_{31}	[Fe/H]	$[Fe/H]_{Layden}$	$\sigma_{[Fe/H]}$
1	0.552281	5.11936	–1.38	–1.65	0.19
5	0.615099	5.40388	–1.42	–1.69	0.28
7	0.588000	5.17437	–1.51	–1.79	0.23
12	0.587633	5.22300	–1.46	–1.73	0.22
14	0.608022	5.85473	–0.91	–1.16	0.20
21	0.612120	4.77138	–2.06	–2.36	0.28
23	0.523110	4.41584	–1.95	–2.25	0.17
24	0.596015	5.74087	–0.96	–1.21	0.38
25	0.800898	5.61235	–2.19	–2.50	0.17
27	0.596109	5.37598	–1.34	–1.61	0.14
34	0.562213	5.42900	–1.11	–1.36	0.15
37	0.598353	5.19618	–1.54	–1.82	0.15
44	0.528236	5.06653	–1.30	–1.57	0.25
45	0.561698	5.32247	–1.21	–1.48	0.15
49	0.547890	5.67561	–0.77	–1.02	0.19
59	0.522958	5.05802	–1.28	–1.55	0.25
71	0.460702	4.76450	–1.26	–1.52	0.16
76	0.577865	4.76634	–1.88	–2.18	0.17
79	0.572610	5.20478	–1.40	–1.67	0.26
97	0.547472	5.27824	–1.18	–1.45	0.25
103	0.483590	4.70712	–1.44	–1.71	0.16
104	0.602988	5.50416	–1.25	–1.51	0.15
109	0.730896	5.36499	–2.08	–2.38	0.15
115	0.554167	5.18484	–1.32	–1.59	0.16
120	0.612234	6.04222	–0.73	–0.98	0.21
121	0.426879	5.66504	–0.14	–0.35	0.30
124	0.561183	5.46345	–1.06	–1.32	0.45
128	0.621765	5.04672	–1.82	–2.11	0.16
134	0.643060	5.33914	–1.63	–1.91	0.14
137	0.609840	5.37539	–1.42	–1.69	0.17
144	0.580523	5.48349	–1.15	–1.41	0.21

Notes: The ID of RR Lyrae star as given in Wu et al. (2005); [Fe/H]: iron abundance calculated from Fourier parameters and in the scale of JK96; $[Fe/H]_{Layden}$: iron abundance in the scale of L94 transformed using the formula of JK96, i.e. $[Fe/H]_{Layden} = ([Fe/H] - 0.200)/0.957$.

relation exists for the W band[4], although Dorfi & Feuchtinger (1999) claimed linear relations among the φ_{31} of the *UBVI* bands by analyzing Fourier parameters based on synthetic multi-color light curves of theoretical models.

Like JK96, we used a linear function to do regression analysis for our *calibrating sample* (31 variables in set #1). We obtained a similar empirical formula in the W band, i.e.

$$[Fe/H] = -3.766 - 5.350P + 1.044\varphi_{31}. \quad (2)$$

The Fourier [Fe/H] obtained using Eq. (2) of data set #1 agree well with that of the spectroscopic [Fe/H], as shown in Fig. 5. The standard deviation is 0.14 dex for the *calibrating sample*, which is consistent with the fitting accuracy of the calibrating set of JK96. The six stars that deviate more than 0.3 dex from the spectroscopic values suffer from problems similar to those described in JK96 and K05. FH Vul, AA Leo, and V341 Aql show the largest deviations from the spectroscopic value. We note that FH Vul and AA Leo have very noisy light curves. For V341 Aql, there is no reasonable explanation for the large deviation (see also JK96). In the sequence of the degree of discrepancy, the next two stars are RX Cet and RY Psc, which are Blazhko stars (see K05). V440 Sgr has insufficient phase coverage.

We suggest that the insufficient-phase-coverage light curves can still be used to predict [Fe/H] to some extent, as long as data

[4] The unfiltered CCD band of ROTSE-I is called the W band.

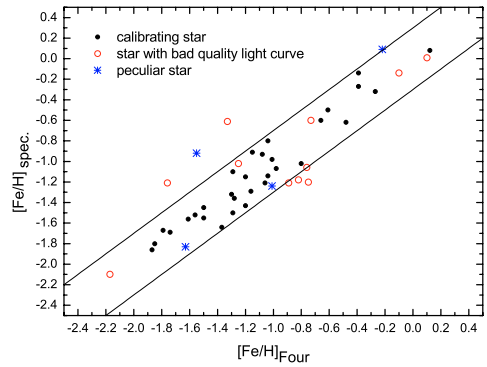

Fig. 5. Spectroscopic versus Fourier [Fe/H] computed for 46 stars of the database set #1. Two lines show the ±0.3 dex boundaries for $[Fe/H]_{Spec.} = [Fe/H]_{Four.}$.

Table 4. Parameters and coefficients of the various linear regressions to the *calibrating sample* (31 variables in set #1).

The relation	SD	R
$[Fe/H] = -3.766 - 5.350P + 1.044\varphi_{31}$	0.139	0.960
$[Fe/H] = 0.603 - 5.375P + 0.636\varphi_{41}$	0.152	0.952
$[Fe/H] = -2.380 - 5.287P + 1.636\varphi_{21}$	0.166	0.940
$[Fe/H] = -0.233 - 4.532P + 0.331\varphi_{51}$	0.169	0.915
$[Fe/H] = 2.100 - 4.694P - 6.925A_3$	0.196	0.897
$[Fe/H] = 2.040 - 4.866P - 8.399A_4$	0.227	0.860
$[Fe/H] = 1.841 - 4.804P - 9.836A_5$	0.230	0.855
$[Fe/H] = 2.140 - 4.618P - 2.663A_1$	0.232	0.853
$[Fe/H] = 1.510 - 4.342P - 1.954A_2$	0.244	0.820

Notes: The relation is derived from the linear regression to the *calibrating sample*, where P is period. The φ_{i1} is defined as $\varphi_{i1} = \varphi_i - i\varphi_1$, and A_i refers to Eq. (1). SD: standard deviation of the fit. R: correlation coefficient.

points around the maximum and minimum phases are not absent. We note that 6 out of the 7 objects of set #1 with insufficient phase coverage do fall into the area enclosed by the ±0.3 dex lines in Fig. 5, except for V440 Sgr. Even the $\Delta[Fe/H]$[5] of V440 Sgr, −0.32 dex, is not very large.

We also compared the metallicity indicator of φ_{31} with the other phases and amplitudes in Table 4. In this table, we list the parameters, standard deviation, and correlation coefficient for various linear formulae in the order of decreasing fitting accuracy. We note that φ_{31} is still the best one for the W band, as well as for the V band. In addition, the phases show distinctively better fits than the amplitudes.

We tested this calibrated relation (Eq. (2)) on data set #2. The results are satisfactory, as shown in Fig. 6, although the scatter is a little larger than in the case of the *calibrating sample*. The on-average lower brightness of set #2 must be responsible for the larger scatter because fainter objects tend to have lower photometric and spectroscopic accuracy. The photometric errors of some faint objects in set #2 are larger than 0.05 mag. So, we increased the cutoff value of $\Delta[Fe/H]$ from ±0.3 to ±0.4, which results in 14 outliers, as listed in Table 5. We use NL to indicate a noisy light curve and IPC those with insufficient phase coverage (this classification is somewhat subjective, but see K05). Variables marked as IS have a standard deviation of the spectroscopic abundance larger than 0.2.

All outliers, except for UY Boo, DG Hya, RZ Cam, and BK And, can be explained by either the bad quality of the light curves (e.g. GY Her, AE Vir, and V964 Ori), the

[5] $\Delta[Fe/H] = [Fe/H]_{Spec.} - [Fe/H]_{Four.}$

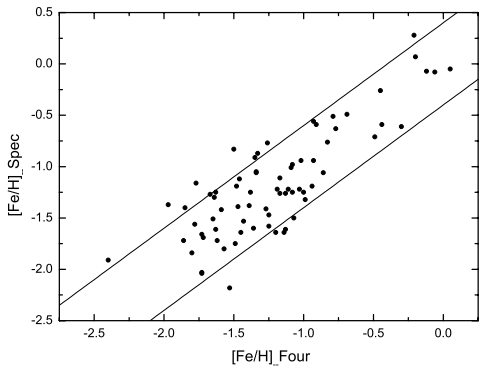

Fig. 6. Spectroscopic versus Fourier [Fe/H] computed for 72 stars of the database set #2. Two lines show the ±0.4 dex boundaries for $[Fe/H]_{Spec.} = [Fe/H]_{Four.}$.

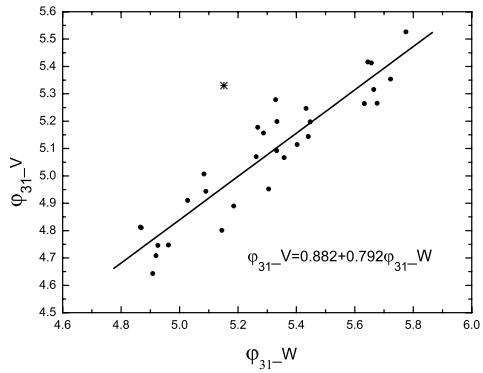

Fig. 7. The relation of φ_{31} between the W and the V bands. The line is a linear fit for the relation. The asterisk is TZ Aur with a deviation of more than 3σ.

Table 5. Outliers in [Fe/H] from set #2.

Variable	Mag	Δ[Fe/H]	Rem
RR CVn	12.9	–0.66	IS
UY Boo	11.3	–0.65	–
DG Hya	12.3	0.62	–
BK Eri	12.9	–0.60	IS
UU Boo	12.6	–0.50	IS
RZ Cam	13.2	–0.49	–
SV CVn	12.8	–0.49	IS, IPC
BK And	13.2	–0.49	–
V964 Ori	13.6	0.48	IPC
SW Boo	12.7	0.46	IS
AW Ser	13.2	–0.45	NL
AE Vir	13.4	–0.44	NL
GY Her	13.0	0.44	IPC
AR Ser	12.2	–0.43	BL, NL

Notes: Mag: the magnitude of ROTSE-I; BL: the Blazhko variable; NL: the noisy light curve. IPC: the light curve with insufficient phase coverage; IS: inaccurate $[Fe/H]_{Spec}$.

presence of the Blazhko effect (e.g. AR Ser), or the possible large errors in spectroscopic abundance (e.g. SW Boo and RR Cvn). For RZ Cam and BK And, we suspect that the real errors of their spectroscopic abundance were larger than those listed in L94 because the numbers of their measurements were not more than 2, and both objects are fainter than 13 mag in the W band. We also note that UY Boo has the lowest metallicity in the sample, which could be responsible for its large discrepancy. However, we cannot find a reasonable explanation for the deviations of DG Hya (see also K05).

The fitting accuracy in our test for the P-φ_{31}-[Fe/H] relation in the W band is comparable to that found by K05 in the test on the ASAS sample for the V-band relation. Including all 72 stars of set #2, we have $\sigma(\triangle[Fe/H]) = 0.29$ dex. Leaving out the 14 outliers listed in Table 5, we get 0.21 dex. If further combined with the *calibrating sample*, the accuracy becomes 0.19 dex.

3.2. Comparison with JK96

To assess the calibration of the JK96 relation and that of our relation, we compare the periods, derived [Fe/H], and φ_{31} for the common stars. The periods of JK96 and ours agree within 1.3×10^{-4} days, including DG Hya. Inspecting the light curves folded with our periods, we notice that most of them are of good or fine quality, in spite of expected large scatter at such faint magnitudes for photometric data obtained with a small telescope. On the other hand, some variables display rather large scatter due to the Blazhko effect or to observational noises (marked by pound signs in Table 1). Except for these noisy light curves, the RMSE values of Fourier fits are all less than 0.06.

The consistency between the derived [Fe/H] values using our W-band relation, $[Fe/H]_{our}$, and those using the JK96 V-band relation, $[Fe/H]_{JK96}$, can be seen in Fig. 8. The solid line in the top panel represents $[Fe/H]_{our} = [Fe/H]_{JK96}$. The bottom panel plots the relation between Δ[Fe/H] and $[Fe/H]_{JK96}$, and $\Delta[Fe/H] = [Fe/H]_{our} - [Fe/H]_{JK96}$. Two dashed lines represent $\Delta[Fe/H] = \pm 0.3$, while the solid line represents $\Delta[Fe/H] = 0$. Circles and triangles are the stars common to JK96, i.e. the whole set #1 and the set #2 stars common to K05, respectively. After discarding the six outliers that have discrepancies larger than 0.3 dex, we can reach a standard deviation of 0.133 dex. All outliers can be explained by the Blazhko effect or noisy light curves. If TZ Aur[6] is also left out, the standard deviation will be decreased to 0.111 for the *calibrating sample*. In comparison to the analysis of K05, we think that this deviation is normal and is likely introduced by photometric and fitting discrepancy. In addition, we can see that the Δ[Fe/H] has no correlation with $[Fe/H]_{JK96}$.

We plot φ_{31} in the V band against that in the W band in Fig. 7, where the difference is ∼5%, in general. The relation of φ_{31} between the W and V bands can be fitted by

$$\varphi_{31\_V} = 0.882 + 0.792\varphi_{31\_W}, \quad (3)$$

with a quadratic correlation coefficient, R^2, of 0.87. We note that a linear relation between the V- and I-band Fourier parameters has been derived by Morgan et al. (1998), using the observational data of Walker (1994). On the theoretical side, Dorfi & Feuchtinger (1999) have shown similar results from model calculations. Therefore, we suggest that Eq. (3) is also physical.

The star TZ Aur (asterisk) lies beyond the 3σ level in Fig. 7. No Blazhko effect has been reported for this star in the GCVS4, and its light curve shown here is very nice. A large deviation also existed in JK96′s calibration, although its highly non-uniformly sampled light curve in that paper might be responsible. So we classify TZ Aur as a peculiar star like V341 Aql and DG Hya. Whether they have a common intrinsic mechanism is beyond the scope of this paper.

[6] An outlier in the relation of φ_{31} between the W band and the V band.

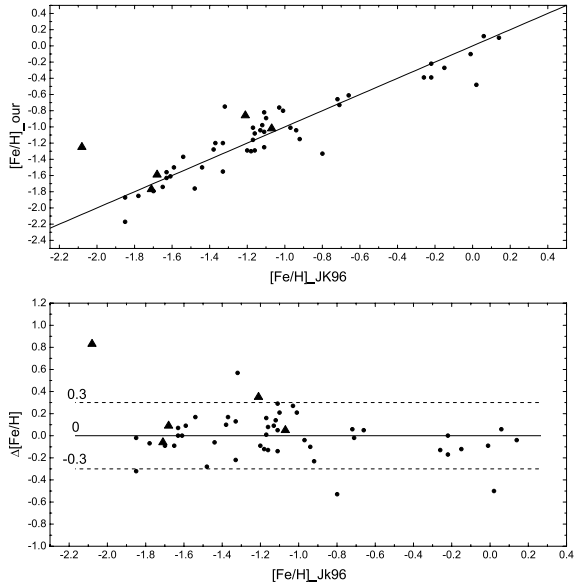

Fig. 8. *Top*: plot of [Fe/H] predicted by JK96 against those of ours for the common star. The solid line indicates $[Fe/H]_{our} = [Fe/H]_{JK96}$. *Bottom*: plot of Δ[Fe/H] versus $[Fe/H]_{JK96}$(Δ[Fe/H] = $[Fe/H]_{our} - [Fe/H]_{JK96}$). Two dashed lines present Δ[Fe/H] = ±0.3 around the Δ[Fe/H] = 0 (solid line). Circles and triangles indicate the common stars in the datasets of JK96 and set #2 of K05, respectively.

4. Predicted [Fe/H] of data set #3

To use our P-φ_{31}-[Fe/H] relation to predict iron abundance, one should pay special attention to the following considerations: (1) Light curves of bad quality must be excluded. From our experience, the light curves with Fourier-fitting RMSE larger than 0.06 and those of insufficient phase coverage, in particular those with a lack of data around the maximum and minimum, cannot be used. In addition, photometric errors are required to be less than 0.05 to meet those of sets #1 and #2. (2) There is a chance of ∼6% of encountering peculiar variables, as demonstrated by sets #1 and #2, which include three unexplained outliers, corresponding to 3%, and the outliers of Blazhko stars, adding another 3%. The ratio of Blazhko stars in RRabs was estimated based on the results of Moskalik & Poretti (2003), Smith (1995), and K05. (3) The unfiltered CCD that is used should have sensitivity similar to that of ROTSE-I, i.e. the W band.

Our data set #3 is ideal for the application of Eq. (2) to predict [Fe/H]. It has photometric errors of less than 0.05 mag (see Wu et al. 2005, Fig. 1a) and RMSE of less than 0.06. Light curves with insufficient phase coverage around the maximum and minimum light are not included. The difference between the sensitivity of the unfiltered CCD of ROTSE-I and that of the W05 system[7] is small (see also Riess et al. 1999). To test this, we selected 5 RRLSs from set #1 and measured their light curves with the W05 system. The stars are listed in Table 6, and their light curves are shown in Fig. 9. We compared our predicted [Fe/H] with their spectroscopic values cited in JK96. The difference is less than 0.14 dex, except for ST Oph, whose light curve lacks data points around the maximum and minimum, although the mechanical shutter effect[8] introduced noises to the light curves of these bright stars. This indicates that Eq. (2) is fit for the W05 system.

Table 6. RRLSs observed with the 0.8-m telescope in the Xinglong Station.

Variable	$[Fe/H]_{Spec}$	$[Fe/H]_{Four}$	Δ[Fe/H]
V452 Oph	–1.45	–1.45	0.00
VX Her	–1.21	–1.21	0.00
KX Lyr	–0.24	–0.21	–0.03
IO Lyr	–1.1	–0.96	–0.14
ST Oph	–1.02	0.31	–1.33

Notes: $[Fe/H]_{Spec}$ and $[Fe/H]_{Four}$ are [Fe/H] derived from the spectrum and by the Fourier method, respectively.

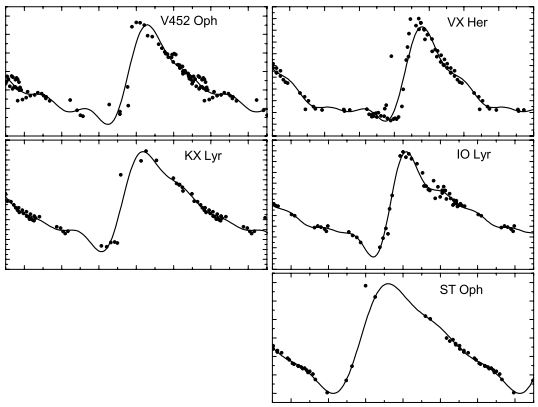

Fig. 9. Light curves of five RRab stars from data set #1 observed by the 0.8-m telescope in the Xinglong Station with an unfiltered CCD.

The predicted iron abundance of set #3 is presented in Table 3. [Fe/H] and $[Fe/H]_{Layden}$ indicate the calculated iron abundance in the scale of JK96 and L94, respectively. To transform between the two scales, we used the formula of JK96, i.e. $[Fe/H]_{JK96} = 0.957[Fe/H]_{Layden} + 0.200$. The errors of [Fe/H] listed in the sixth column were calculated by the following formula:

$$\sigma^2_{[Fe/H]} = 1.089\sigma^2_{\varphi_{31}} + 2K_{12}P + 2K_{13}\varphi_{31} + 2K_{23}P\varphi_{31} + K_{11} + K_{22}P^2 + K_{33}\varphi^2_{31}, \quad (4)$$

where the coefficients have the values

$$K_{12} = -0.00884 \quad K_{13} = -0.01426 \quad K_{23} = -0.00301$$
$$K_{11} = 0.08061 \quad K_{22} = 0.04584 \quad K_{33} = 0.00300. \quad (5)$$

The error in the period is also omitted as in Eq. (4) of JK96. The regression coefficients of K_{ij} ($i \neq j$) are caused by the non-orthogonality of the regression variables P and φ_{31} on the calibrating data set. The mean value of $\sigma_{[Fe/H]}$ is ∼0.21 dex.

The method that we used to predict [Fe/H] needs further checks to ensure its validity because it is based on an empirical statistical relation that, so far, has no physical interpretation (K05) and because it strongly depends on the quality of light curves. Therefore, we make the following comparisons between our results and those in the literature:

(1) We plot the histogram of the [Fe/H] values of set #3 in Fig. 10. The distribution of the [Fe/H] is at $\sigma = 0.45$ around a mean value of −1.63[9]. It is consistent with that derived from the BHB stars in the Milky Way's halo by Kinman et al. (2000), which has a mean [Fe/H] of −1.67 with a dispersion of 0.42.

[7] An unfiltered CCD mounted on the 0.8-m telescope in the Xinglong Station.

[8] The time of moving the mechanical shutter can cause one side of the field to be exposed longer than the other.

[9] In the scale of L94.

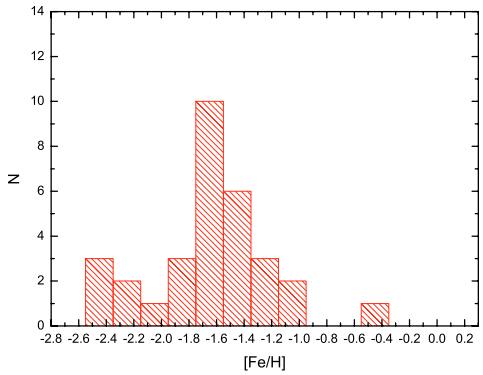

Fig. 10. Histogram of the [Fe/H] of set #3.

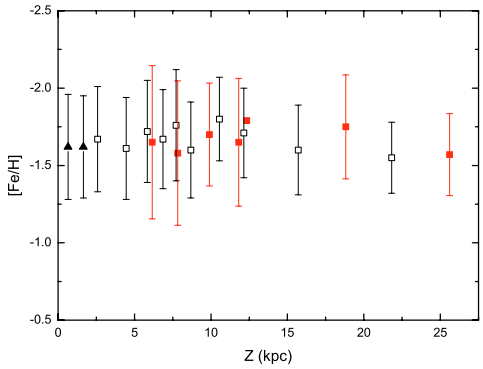

Fig. 11. Plot of the predicted [Fe/H] vs. distance (Z) from the galactic plane. The solid squares are the mean [Fe/H] of set #3 in the bin of 2 kpc, and the open squares indicate data from Suntzeff et al. (1991). Triangles are the data from Table 10 in L94. Their [Fe/H] are all converted to the same scale as L94. The error bars indicate the standard error of the mean in each abundance bin.

(2) We re-plot the mean [Fe/H] values against the distance from the Galactic plane, Z, for the data of L94 and Suntzeff et al. (1991), adding our mean [Fe/H] of set #3 binned in 2kpc for comparison. For $Z \leq 12$ kpc, our results are consistent with those of Suntzeff et al. (1991). Du et al. (2004) also found a similar trend of [Fe/H] vs. Z using the photometric data of F/G dwarfs. L94 has argued that there is no gradient within 3 kpc based on his comparison with the data of Suntzeff et al. (1991), which is again in agreement with our results. For $Z > 12$ kpc, the trend of richer metal for a larger Z in L94 is also present in our data (see L94 for a possible physical explanation), although our sample has slightly lower metallicity than that in L94.

The consistency between the mean [Fe/H] of set #3 and that of Kinman et al. (2000) indicates that it is reasonable for Vivas et al. (2005) to use the result of Kinman et al. (2000) to distinguish the Sgr stream because the Galactic halo stars of set #3 are closer to the Sgr stream than the stars of Kinman et al. (2000) in spatial distribution (Ivezić et al. 2000).

We found that the eight stars (see Table 7), whose distances to star 91[10] are less than 3 kpc, have a mean metallicity, i.e. −1.79, lower than the average value, −1.63. Moreover, if the distance criterion is reduced to 2 kpc and 1 kpc, the mean [Fe/H] for the remaining stars becomes −1.75 and −1.84, respectively. W05 have pointed out that star 91 is a lower-metallicity and large-mass double-mode RR Lyrae star, based on its position in the Petersen diagram. The fact that both star 91 and its near variables have low metallicity indicates that they may have a common origin. This supports the suggestion made by W05 that star 91 is in tidal debris of a globular cluster of the Galaxy or from a dwarf galaxy.

We note that stars 120 and 121 have abundances of −0.98 and −0.35, respectively. The synthetic HB model is difficult to use to reproduce these values (Lee 1992), and these stars are unlikely members of metal-rich globular clusters (L94 and references therein). According to Taam et al. (1976), they may originate from a small fraction of the progenitor giant stars that experienced enhanced mass loss.

[10] Refer to W05.

Table 7. RRLSs in the range of 3 kpc to star 91.

ID	D(kpc)	[Fe/H]$_{\rm Layden}$
76	0.68	–2.18
104	0.74	–1.51
59	1.81	–1.55
71	2.14	–1.52
115	2.41	–1.59
109	2.75	–2.38
97	2.96	–1.45
128	2.98	–2.11

Notes: ID, as given in Wu et al. (2005); D: the distance from star 91; [Fe/H]$_{\rm Layden}$: as given in Table 3.

5. Summary

We extend the P-φ_{31}-[Fe/H] relation of JK96 in the V band to the W band, based on the photometric data of ROTSE-I and spectroscopic [Fe/H] of JK96 and L94. The calibrated relation of the W band, [Fe/H] $= -3.766 - 5.350P + 1.044\varphi_{31}$, has an accuracy of 0.14 dex for the *calibrating sample* (31 stars) and 0.21 dex for the test sample of 58 stars (free of outliers). When the two samples are combined, the value becomes 0.19 dex. These accuracy values are in agreement with that of the similar formula in the V band for the test by K05.

We also find an empirical relation of φ_{31} between the V and W bands, i.e. $\varphi_{31\_V} = 0.882 + 0.792\varphi_{31\_W}$, which is similar to the linear one determined by Morgan et al. (1998) for the V and I bands, using the observational data of Walker (1994). On the theoretical side, Dorfi & Feuchtinger (1999) have shown similar results between the V and I bands from model calculations. So, we suggest that this linear relation between the V and W bands is also physical.

Although the above result is satisfactory in terms of the dispersion between the computed and measured metallicities, the physical cause of these relations is not clear. To use our P-φ_{31}-[Fe/H] relation to predict iron abundance, one should consider three aspects in processing the data: (1) light curves of bad quality must be excluded. From our experience, the light curves with Fourier-fitting RMSE larger than 0.06 and those of insufficient phase coverage, in particular a lack of data around the maximum and minimum, cannot be used. In addition, photometric errors are required to be less than 0.05 mag. (2) There is a chance of ∼6% of finding peculiar variables, which cannot be avoided in [Fe/H] prediction. (3) The unfiltered CCD that is used should have a sensitivity similar to that of ROTSE-I, i.e. the W band.

Based on these considerations, we selected 31 RRab stars (set #3) in the W05 sample and predicted their [Fe/H] using our P-φ_{31}-[Fe/H] relation. Comparisons between our result and those in literatures indicate that our results are reliable, although

the method is based on an empirical statistical relation and strongly depends on the quality of the light curves.

We obtain characteristics of halo RRLSs from our predicted [Fe/H] as follows. (1) The mean [Fe/H] value of our halo RRLSs is −1.63 with a dispersion of 0.45 in distribution. This indicates that it is reasonable for Vivas et al. (2005) to use the result of Kinman et al. (2000) to distinguish the Sgr stream because the Galactic halo stars of set #3 are closer to the Sgr stream than the stars of Kinman et al. (2000) in spatial distribution (Ivezić et al. 2000). (2) The fact that both star 91 (a double-mode RRLS) and its near RRLSs have low metallicity indicates that they may have a common origin. This supports the suggestion made by W05 that star 91 is a tidal debris of a globular cluster of the Galaxy or of a dwarf galaxy. (3) Two RRLSs have the value of [Fe/H] of −0.98 and −0.35. The synthetic HB model to reproduce these values is difficult (Lee 1992), and these stars are unlikely members of metal-rich globular clusters (L94 and references therein). According to Taam et al. (1976), they may originate from a small fraction of the progenitor giant stars that experienced enhanced mass loss.

Acknowledgements. We would like to thank the anonymous referee for valuable comments. We are grateful to G. Kovàcs for useful suggestions. We thank A. L. Lou and Y. X. Zhang for useful discussions. A. K. Vivas is greatly acknowledged for providing us with the *V*-band photometric data of the RRLSs.

References

Dorfi, E. A., & Feuchtinger, M. U. 1999, A&A, 348, 815
Durlevich, O. V., et al. 1994, The list of errors in the GCVS, 4th edition
Du, C. H., Zhou, X., Ma, J., et al. 2004, AJ, 128, 2265
Feuchtinger, M. U. 1999, A&A, 351, 103
Ivezić, Ž., Goldston, J., Finlator, K., et al. 2000, AJ, 120, 963
Jurcsik, J., & Kovács, G. 1996, A&A, 312, 111 (JK96)
Kholopov, P. N. 1988, General Catalogue of Variable Stars, 4th edn., Vols. I–III (Moscow: Nauka) (GSCV4)
Kinman, T. D., Castelli, F., Cacciari, C., et al. 2000, A&A, 364, 102
Kovács, G. 2005, A&A, 438, 227 (K05)
Kovács, G., & Zsoldos, E. 1995, A&A, 293, L57
Kovács, G., & Kanbur, S. M. 1998, MNRAS, 295, 834
Layden, A. C. 1994, AJ, 108,1016 (L94)
Lee, Y.-W. 1992, AJ, 104, 1780
Morgan, S. M., Simet, M., & Bargenquast, S. 1998, Acta Astron., 48, 341
Moskalik, P., & Poretti, E. 2003, A&A, 398, 213
Newberg, H. J., Yanny, B., Rockosi, C., et al. 2002, ApJ, 569, 245
Odenkirchen, M., Grebel, E. K., Rockosi, C. M., et al. 2001, ApJ, 548, L165
Pojmanski, G. 2002, Acta Astr., 52, 397
Pojmanski, G. 2003, Acta Astr., 53, 341
Pojmanski, G., & Maciejewski, G. 2004, Acta Astr., 54, 153
Riess, A. G., Filippenko, A. V., Li, W., et al. 1999, AJ, 118, 2675
Sandage, A. 2004, AJ, 128, 858
Simon, N. R., & Lee, A. S. 1981, ApJ, 248, 291
Simon, N. 1988, ApJ, 328, 747
Stellingwerf, R. F. 1978, ApJ, 224, 953
Smith, H. A. 1995, RR Lyrae stars (Cambridge: Cambridge Univ. Press)
Suntzeff, N. B., Kinman, T. D., & Kraft, R. P. 1991, ApJ, 367, 528
Taam, R. E., Kraft, R. P., & Suntzeff, N. B. 1976, ApJ, 207, 201
Vivas, A. K., & Zinn, R. 2003, Mem. Soc. Astron. It., 74, 928
Vivas, A. K., Zinn, R., Andrews, P., et al. 2001, ApJ, 554, L33
Vivas, A. K., Zinn, R., Abad, C., et al. 2004, AJ, 127, 1158
Vivas, A. K., Zinn, R., & Gallart, C. 2005, AJ, 129, 189
Walker, A. 1994, AJ, 108, 555
Wetterer, C. J., & McGraw, J. T. 1996, AJ, 112, 1046
Woźniak, P. R., Vestrand, W. T., Akerlof, C. W., et al. 2004, AJ, 127, 2436
Wu, C., Qiu, Y. L., Deng, J. S., Hu, J. Y., & Zhao, Y. H. 2005, AJ, 130, 1640 (W05)
Yanny, B., Newberg, H. J., Kent, S., et al. 2000, ApJ, 540, 825
Yanny, B., Newberg, H. J., Grebel, E. K., et al. 2003, ApJ, 588, 824
Zinn, R., Vivas, A. K., Gallart, C., & Winnick, R. 2004, ASPC, 327, 92

Online Material

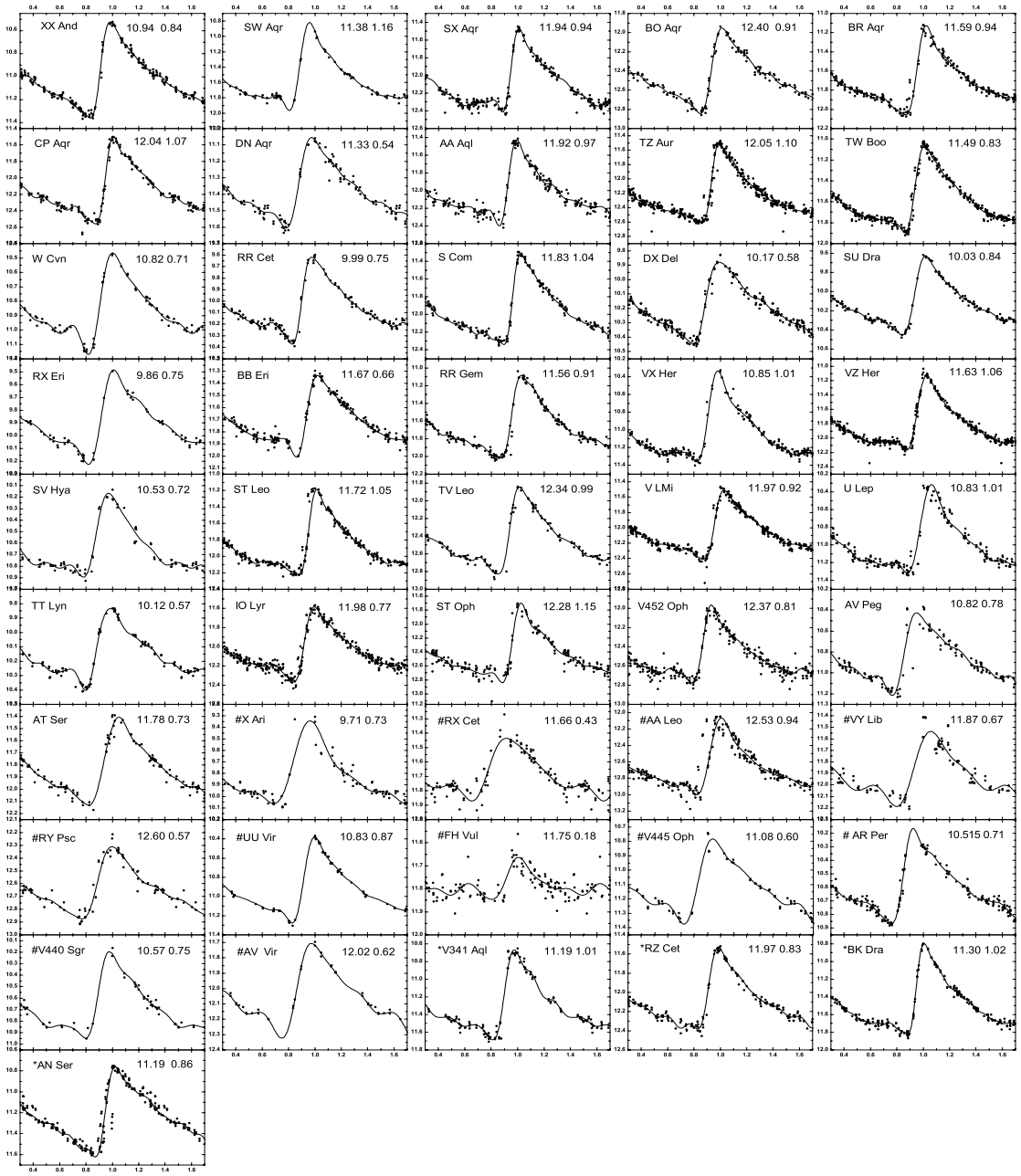

Fig. 1. Folded light curves from the ROTSE-I database. All variables also appear in the compilation of JK96. The orders of the Fourier fits were determined from the SNR of the light curves, as described in the text. *Headers*: Name, average brightness in *W* band, and total amplitude [mag] of the fitted light curve (continuous line). The light curves are plotted in the 1.4 phase interval.

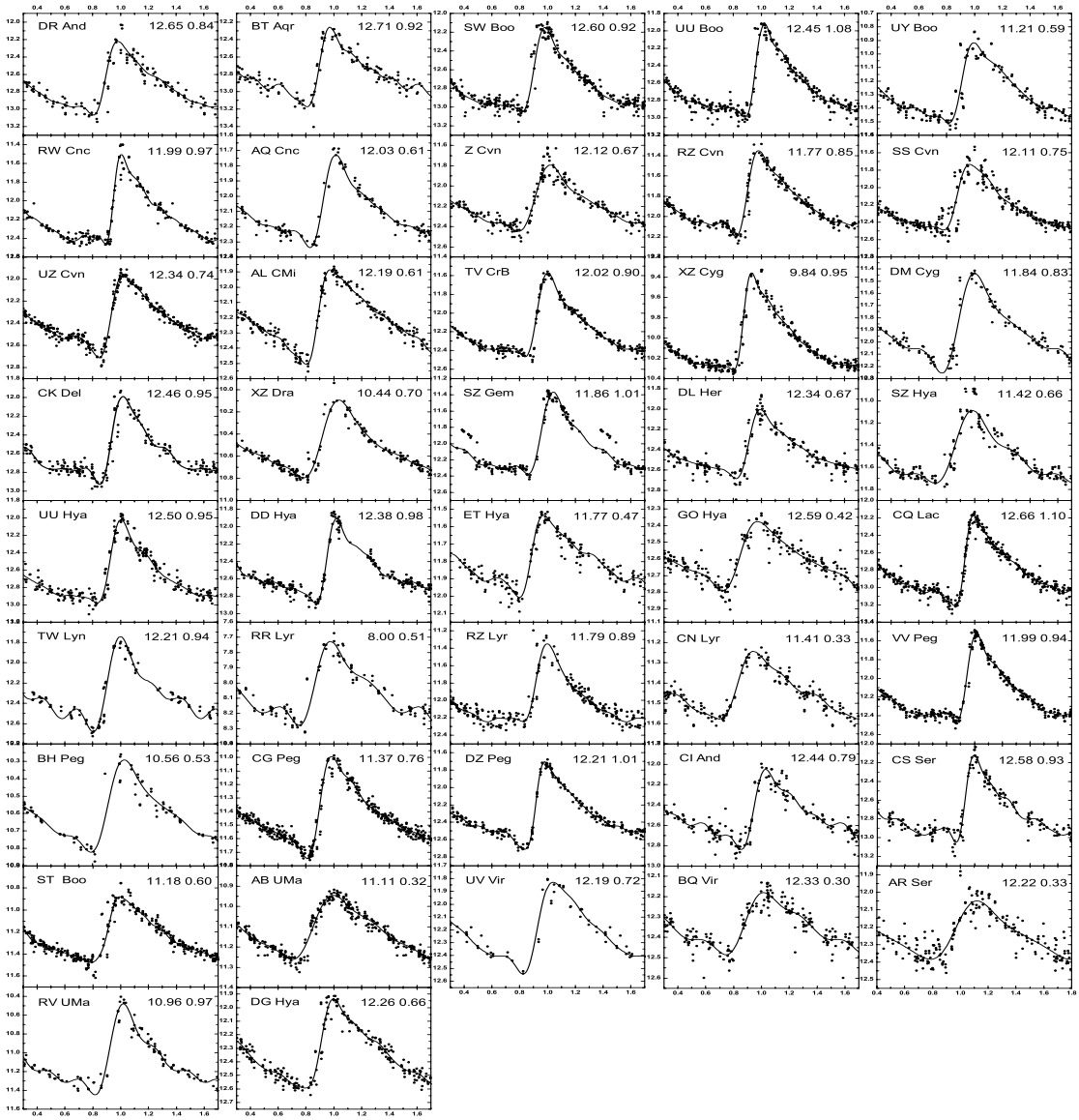

Fig. 2. Folded light curves from the ROTSE-I database. None of the variables is contained in the compilation of JK96, but all have low-dispersion spectroscopic metallicities from L94. The notation is the same as in Fig. 1.

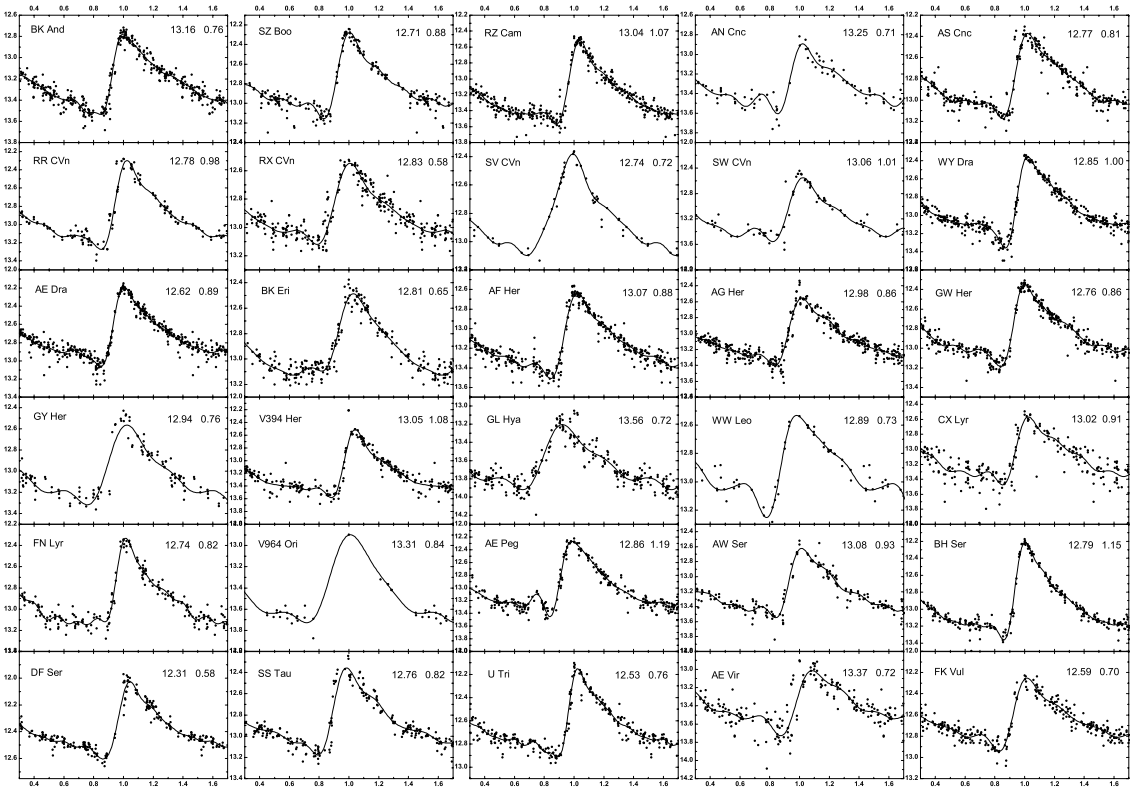

Fig. 3. Folded light curves from the ROTSE-I database. Data selection and notation are the same as in Fig. 2.

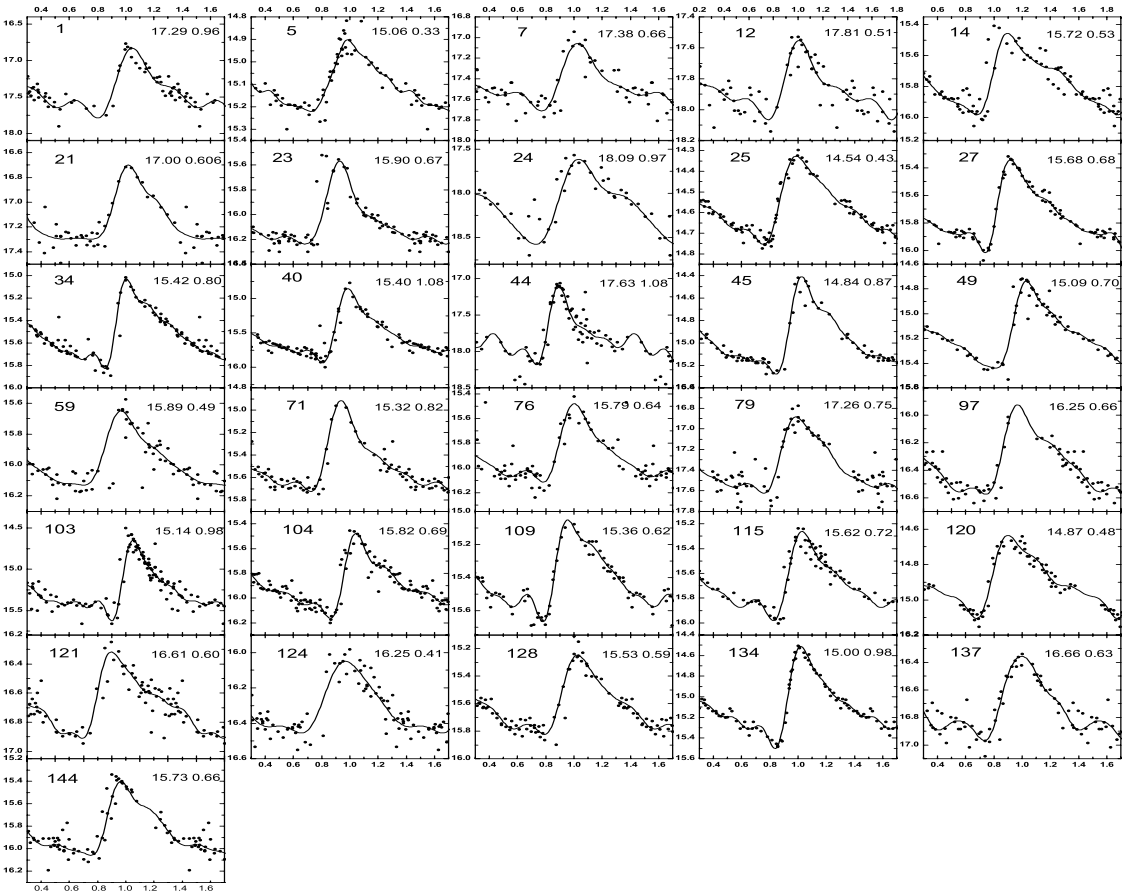

Fig. 4. Light curves of 31 RRab variables from W05. *Headers*: ID of the star (as given in Wu05), average brightness in the band of the W05 system (see footnote 7), and total amplitude [mag] of the fitted light curve (continuous line). The light curves are plotted in the 1.4 phase interval.